PHYSICAL REVIEW E VOLUME 57, NUMBER 6 JUNE 1998

Magnetic-field induced orientation and anisotropic susceptibility of normal alkanes

Henry H. Shao, Hu Gang, and E. B. Sirota*
Corporate Research Science Laboratory, Exxon Research and Engineering Company, Route 22 East, Annandale, New Jersey 08801
(Received 15 December 1997)

Nonfunctionalized *n*-alkanes, a basic organic building block, are not commonly associated with magnetic behavior. To quantify magnetic field effects on wax crystals, synchrotron x-ray scattering was used to measure the angular distribution arising from competition between Brownian rotation and magnetic energy in a dispersion of uniform-sized *n*-alkane single crystals. Dramatic alignment of both axes occurred with a preference of the carbon-backbone plane to be $\perp$ to $\vec{H}$. Diamagnetic anisotropies were obtained by quantitative analysis of the orientational distribution. [S1063-651X(98)50106-7]

PACS number(s): 61.30.Gd, 61.43.−j, 61.66.Hq

Normal alkanes, CH_3-$(CH_2)_{n-2}$-CH_3, (C_n), are among the most basic organic molecules and are building blocks of many other materials including lipids, surfactants, and polymers, and are themselves the main component of petroleum waxes. Many physical properties of the derivative molecules are dominated by those of the alkyl chains. While the properties of alkanes have been known for a long time [1–3] new and unexpected phenomena with respect to structural and thermodynamic properties of the bulk and surface continue to be discovered [4–8]. The fundamental importance of the alkanes makes the detailed characterization and understanding of their behavior a priority.

Functionalized molecules with alkyl chains can often be aligned using magnetic fields. This is especially true for liquid crystals, whose diamagnetic anisotropy is usually strongly dominated by the aromatic rings [9]. Magnetic fields are, however, also used to align phospholipids [10–12] where the alkyl chains play a more significant role. The interaction of the magnetic fields with alkane crystals themselves is also of current interest in the petroleum industry, where suggestions that ''magnetic conditioning'' can control wax deposition problems abound [13].

While often extremely weak, diamagnetism exists in all materials and will be dominant when ferro- and paramagnetic effects are absent. The average diamagnetic susceptibility for liquid —CH_2— chains was determined to be $-\chi = 6.4\times10^{-7}$, in dimensionless units [14]. We will hereafter drop the minus sign since we will exclusively be considering diamagnetic phenomena. Structurally anisotropic molecules will also be diamagnetically anisotropic. It is an anisotropy of the susceptibility that will be responsible for orienting materials in the field. Diamagnetic anisotropy will typically not be sufficient for orienting individual molecules in the liquid phase since the magnetic energy would have to be $\sim k_BT$/molecule, which cannot be easily obtained. An extremely small perturbation to random orientation can be measured through coupling with optical anisotropy (Cotton-Mouton effect), thus providing information on the diamagnetic anisotropy in the liquid phase, and together with other techniques, have been used to compute bond anisotropies [15–17]. Magnetic orientation can be dramatically enhanced by cooperative alignment of molecules as occurs in nematic liquid crystals, lamellar membranes, or crystalline phases [9].

At temperatures (T) below melting, alkanes undergo a number of solid-solid transitions through a series of rotator phases [4–7], which lack long-range order with respect to the rotation of the molecule about its long axis. These phases are characterized by large T-dependent strains which make them particularly interesting but require that properties be measurable as a function of T. Unfortunately, it is difficult to obtain large single crystals which maintain their perfection through the large structural changes. Classic measurements of diamagnetic anisotropies involved measuring the torsional vibrations on a macroscopically large single crystal in a magnetic field [18]. While other organic chain molecules have been studied [11,12,18] the problem of producing sufficiently large perfect single crystals of the *n*-alkanes prevented their measurement.

In this work, we employ monodisperse *n*-alkane droplets [19] suspended in water, which form a dispersion of uniform-sized single-domain crystals when cooled. Because the particles undergo freely rotating motion, the orientational distribution is determined by a balance between random rotation and the orienting force of the magnetic field [11]. We measure the orientational distribution using synchrotron x-ray scattering which lets us quantify the anisotropic diamagnetic susceptibilities. The crystals exhibit alignment both along and normal to the chain axis and we show that the plane of the carbon-carbon bonds tend to orient $\perp$ to the field.

The synchrotron x-ray experiments were carried out at the National Sychrotron Light Source (NSLS) on Exxon's beamline X10A. The magnetic field $\vec{H}$ was applied horizontally, $\perp$ to the direction of the incident x rays. The incident x-ray beam was defined by a pair of Ge(111) crystals ($\lambda = 1.240$ Å) and slits, giving a spot size at the sample of 0.5 mm (vertical)$\times$1 mm (horizontal). The accessible range in scattering-vector **q** was controlled by adjusting the distance between the sample and the Mar image plate area detector. The magnet cell [20] contains a pair of small permanent magnets that generate a uniform magnetic field between the pole pieces. The field could be varied up to 19 000 G by adjusting the gap and/or changing pole pieces. The sample

*Author to whom correspondence should be addressed. Electronic address: ebsirot@erenj.com

was contained in a 2-mm-diam quartz capillary inserted into a temperature controlled copper tube, which has small Kapton covered holes through which x rays can pass.

Highly monodisperse samples were obtained by preparing oil in water emulsions of the liquid *n*-alkanes and the surfactant sodium dodecyl sulfate and then separating by droplet size using a repeated fractionation technique [19]. The SDS concentration in the H_2O phase was 0.01 M, and the volume fraction of alkane was 15%. C_{16} and C_{17} were obtained from Sigma Chemical. The droplet size distributions were measured by dynamic light scattering (DLS) [21] giving polydispersities of $<10\%$. Due to the small size of the droplets, the alkanes crystallize through homogeneous nucleation when cooled $\sim 15\,^{\circ}\mathrm{C}$ below the melting temperature, with each droplet forming a single crystal [3]. Once crystallized, the crystal structures are the same as the bulk alkane samples, showing that SDS and H_2O do not enter and modify the crystal.

Our most detailed measurements were on a C_{16}:C_{17} 50:50 mixture at 10 °C. The mixture melts at $T_m = 19\,^{\circ}\mathrm{C}$ and has a R_I rotator phase extending down to $-6\,^{\circ}\mathrm{C}$ where it transforms to an orthorhombic crystal. This rotator phase is a 3D crystal with the molecules oriented normal to the layers and packed in an orthorhombic structure, with local herringbone order of the carbon backbone planes resembling that of the lower temperature orthorhombic crystal [5,7]. Figure 1(a) is the scattering pattern in the absence of a magnetic field, of the low-**q** range covering the 001 reflection at $\mathbf{q} = 0.2719\ \text{Å}^{-1}$ from the layer spacing $d = 2\pi/\mathbf{q} = 23.1$ Å. It shows a ring with uniform angular distribution since the crystalline droplets freely rotate like Brownian particles. A dramatic alignment of the layer normal is shown in Fig. 1(b), where upon application of the magnetic field $\vec{H}$, the scattering intensity concentrates around $\theta = 90°$ with respect to the field. Since the field only breaks symmetry in one direction, there can be no orientation with respect to rotation of the sample about the horizontal axis. The azimuthal width of the peak, which depends on the volume of the crystal (V), reflects the ratio of the magnetic to the thermal energy. The magnetic energy of a single crystal is $E = V\vec{H}\cdot\vec{\chi}\cdot\vec{H}/2 = VH^2(\chi_c\cos^2\theta + \chi_b\sin^2\theta\cos^2\phi + \chi_a\sin^2\theta\sin^2\phi)/2$ where $\chi_a < \chi_b < \chi_c$ are the three dimensionless principal diamagnetic susceptibilities, θ is the angle between $\vec{H}$ and the χ_c axis (which is along the molecular chain), and ϕ is the angle of rotation about that axis (with $\phi \equiv 0$ when χ_b is along $\vec{H}$). These χ are defined to be positive, since we are exclusively considering diamagnetic phenomena. In thermal equilibrium, the orientational distribution probability can be written as

$$P(\theta) \propto \exp(-E/k_BT) \propto \exp(-VH^2\Delta\chi\cos^2\theta/2k_BT) \times \exp(-VH^2\Delta\chi'\sin^2\theta\cos 2\phi/4k_BT).$$

There are two orientation dependent terms, the first arising from the longitudinal anisotropy ($\Delta\chi \equiv \chi_c - (\chi_a + \chi_b)/2$) and the second from the transverse anisotropy ($\Delta\chi' \equiv \chi_b - \chi_a$). The scattering intensity distribution of the lamellar (001) reflections $I(\theta) \propto P(\theta)$. Thus for $\vec{H} = 0$, $P(\theta)$ will be flat and will develop a 180° modulation for finite $\vec{H}$, becoming strongly peaked at $\theta = \pm 90°$ when $VH^2\Delta\chi/2k_BT \gg 1$ as shown in Fig. 2(a). From the 001 intensity distribution we can thus determine $\Delta\chi$, and from the high-**q** reflections we can determine $\Delta\chi'$.

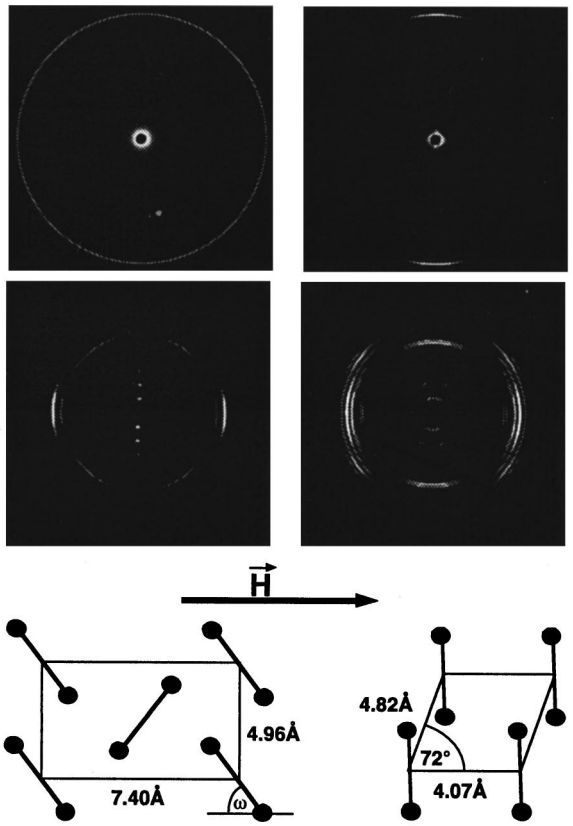

FIG. 1. Two-dimensional scattering patterns for the low **q** range ($0.01 \leq |\mathbf{q}| \leq 0.29\ \text{Å}^{-1}$) showing the 001 reflection for 0.95 μ diameter colloids of C_{16}:C_{17} at 10 °C for (a) $H = 0$ and (b) $H = 10^4$ G. The uniform ring dramatically sharpens in the field. (c) Wide angle ($0.1 \leq |\mathbf{q}| \leq 1.9\ \text{Å}^{-1}$) pattern at $H = 19\,000$ G. The scattering intensity shows a distorted six fold symmetry reflecting the in-plane molecular packing typical of the R_I phase. The six high angle reflections are oriented such that the doubly degenerate higher **q** reflection is oriented along the field while the fourfold degenerate reflections are spaced at $\sim 60°$. A series of oriented 001 reflections can also be observed. (d) Wide angle scattering pattern of the C_{16} triclinic structure at 10 °C, $H = 12\,000$ G with 0.95 μm colloids. The 001 reflections are split off axis. (e) Schematic showing the local packing and orientation of the backbone with respect to the magnetic field in the R_I orthorhombic rotator phase ($\omega > 45°$) and in the triclinic crystal phase.

$P(\theta)$ is predicted above to depend on V and $|\vec{H}|$ in a particular way. To verify this, we prepared samples of the C_{16}:C_{17} mixture with three diameters (0.64, 0.71, and 0.95 μ, each with $<10\%$ polydispersity) and measured $I(\theta)$ for fields varying from 800 to 12 000 G. The kinetic response to changing the field was faster than our 5 min time between data acquisitions and the orientation was reversible on reduction of the field. We fit the $I(\theta)$ data to the above form, with an additional integral accounting for the polydispersity of the size, and obtained excellent agreement, as shown in Fig. 2(a). $I(\theta)$ was found to be the same for higher harmonics of the 001 reflection, as expected. In Fig. 2(b) we show the fitted parameter $\sigma \equiv VH^2\Delta\chi/2k_BT$ plotted vs VH^2. All data fall on a straight line with a slope of unity showing the

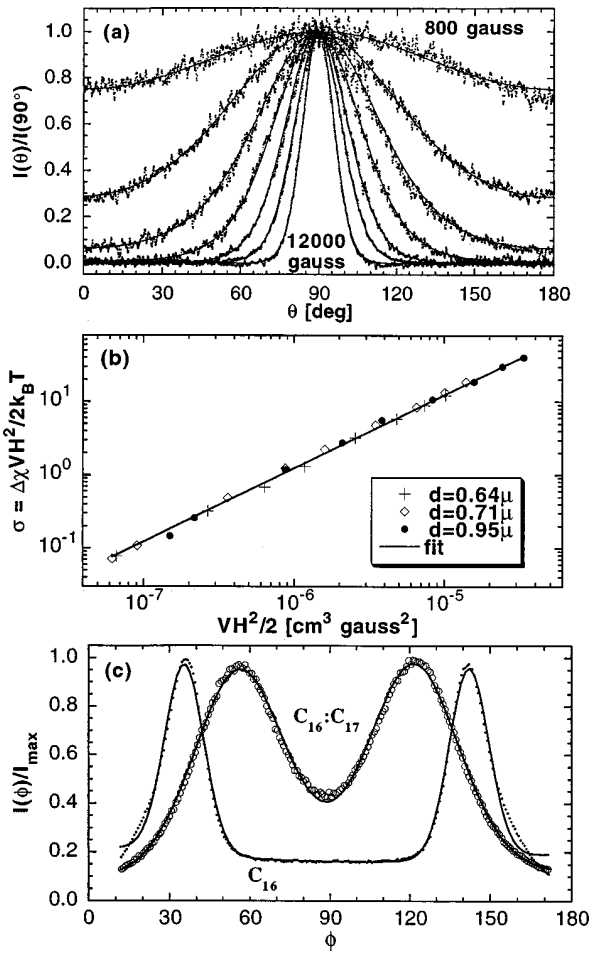

FIG. 2. (a) Circular scans extracted from the 2D data at the 001 peak position ($\mathbf{q}=0.2719$ Å^{-1}), for the 0.95 μm diam sample of C_{16}:C_{17} at 10 °C at fields of 800, 2000, 3000, 4000, 6000, 8000, and 12 000 G. Background has been subtracted and the intensities at $\theta=90°$ have been normalized to unity for ease of presentation. The solid lines are fits to the form in the text for $P(\theta)$, with a Gaussian convolution for the polydispersity in size. (b) A logarithmic plot of the fitted parameter representing the inverse peak width, $\sigma = VH^2\Delta\chi/2k_BT$ vs VH^2, measured for several fields between 800 and 12 000 G on C_{16}:C_{17} with three diameters (0.95, 0.71, 0.64 μ). All data fall nearly on the same straight line with a slope of unity. (c) Circular scans of the high angle peaks at 10 °C, $H=19\,000$ G and fits to the form described in the text. (circles) C_{16}:C_{17}, 0.95 μ at $\mathbf{q}=1.49$ Å^{-1}. Peaks are at $\phi=56°$ and 124° and this fit yields $\Delta\chi'=0.28\times10^{-8}$. (dots) C_{16}, 0.95 μ at $\mathbf{q}=1.753$ Å^{-1}. Peaks are at $\phi=38°$ and 142° and the fit yields $\Delta\chi'=1.5\times10^{-8}$.

scaling of the alignment with field and particle size according to the above relations, which should hold for any noninteracting diamagnetic microcrystal dispersion. From the fitted σ we determine $\Delta\chi=(4.9\pm1.4)\times10^{-8}$ [22]. This is about 40% less than the value for infinite perfectly packed chains obtained from reported bond anisotropies [17]. The T dependence of $\Delta\chi$ in the R_I phase measured between 3 °C and 14 °C was $(1/\Delta\chi)d(\Delta\chi)/dT=-0.01$ °C^{-1}.

In Fig. 1(c) we show the scattering pattern for the high-$\mathbf{q}$ range of the orthorhombic R_I phase at high field. Multiple harmonics of the 001 reflection are aligned at $\theta=90°$. The in-plane reflections associated with the orthorhombic structure are also aligned, albeit not as sharply as the 001 peaks. The peak at $\mathbf{q}\approx1.65$ Å^{-1} is located at $\phi=0°$ and the peaks at $\mathbf{q}\approx1.49$ Å^{-1} are located nearly 60° apart. Since the 2D diffraction pattern is a powder with respect to rotation about the direction of $\vec{H}$, θ and ϕ are mapped onto the same 2D image. This results in an in-plane structure oriented such that the direction of lattice compression is along the magnetic field, as shown schematically in Fig. 1(e). Using the above equation the shape of the in-plane peaks gives us $\Delta\chi'$. Due to the powder average about $\vec{H}$, there is a nearly singular geometrical enhancement of scattering at $\phi=0$ ($\sim\sin^{-1}\phi$) necessitating the use of the off-axis reflections for analysis. A fit to the distribution of the $\mathbf{q}=1.49$ Å^{-1} peak is shown in Fig. 2(c). Data for various fields and sizes yield $\Delta\chi'=(2\pm1)\times10^{-9}$ or $\Delta\chi'/\Delta\chi=0.04$. Since $\Delta\chi'$ is small, it must be extracted from the amplitude of oscillation as opposed to the peak width, and is thus very sensitive to the background level, causing the large uncertainty. The T dependence in the R_I phase is $(1/\Delta\chi')d(\Delta\chi')/dT=-0.04$ °C^{-1}.

Pure C_{16} crystallizes into a triclinic structure, where the molecules are tilted by 19.4° and their backbone planes are packed in a $\parallel$ configuration [23]. This is a more geometrically complicated situation because of the tilt, since orientation of the molecular long axis $\perp$ to $\vec{H}$ allows the 001 scattering to be anywhere in a 40° wide region centered at $\theta=90°$. The 001 peak is only further sharpened by the orientation of the in-plane directions. The diffraction pattern for a magnetically oriented C_{16} sample is shown in Fig. 1(d). The 001 reflections at multiples of $\mathbf{q}=0.305$ Å^{-1} are oriented symmetrically off-axis by $\approx19°$. The strongest in-plane reflections are at $\mathbf{q}=1.374$ Å^{-1}, $\phi=85°$; $\mathbf{q}=1.658$ Å^{-1}, $\phi=8.5°$; and $\mathbf{q}=1.753$ Å^{-1}, $\phi=37.7°$, indexable respectively as 010, 100, and 111. Comparing this to the crystal structure [23] shown in Fig. 1(e), we find that the magnetic alignment places the plane containing the carbon atoms $\perp$ to $\vec{H}$. The shape of the $\mathbf{q}=1.753$ Å^{-1} peak is shown in Fig. 2(c) and fitting various fields and sizes yields $\Delta\chi'=(1.2\pm0.4)\times10^{-8}$. Comparing $\Delta\chi'$ in the two phases we see that in the triclinic it is 6 ± 2 times larger than in the orthorhombic R_I.

In the orthorhombic packing shown in Fig. 1(e), the backbone planes are not $\parallel$, however, they are not exactly $\perp$ to each other. The setting angle of the carbon backbone plane as determined from previous crystallographic investigations is $>45°$ [2]. Thus, the orientation observed here [Fig. 1(c)], as in the triclinic [Fig. 1(d)], shows that the plane containing the carbon atoms tends to orient $\perp$ to $\vec{H}$. Since the diamagnetic interaction tends to align the greatest susceptibilities $\perp$ to $\vec{H}$, the direction with the lowest χ will align along $\vec{H}$. In the case of the alkanes, the greatest χ is along the chain axis and we have shown here that the lowest is $\perp$ to the plane that contains the carbon atoms. Approximating that the diamagnetic anisotropy can be obtained by summing the anisotropies of the individual bonds [16,17] (here C-C and C-H), for an elongated saturated hydrocarbon chain one will obtain the largest susceptibility along the chain axis and the weakest $\perp$ to the C-C plane, with $\Delta\chi'=2\Delta\chi/3$. This is qualitatively consistent with our observations; however, if $\Delta\chi$ for C_{16} is comparable to that in the rotator phase, then $\Delta\chi'/\Delta\chi=0.24$, which is $\ll\frac{2}{3}$. Clearly the nature of the inter- and intramolecular disorder in the crystal phases can be respon-

sible for modifying these values. It is however also possible that the packing of these molecules in a three-dimensionally anisotropic crystalline lattice causes additional perturbation to the electron orbitals which could modify the diamagnetic anisotropies from those expected by summing the anisotropies of independent molecules in the all-trans configuration. Such determinations will require more detailed measurements as a function of chain-length and T.

The strong decreasing $\Delta\chi'$ with increasing T in the rotator phase can be attributed to the strong decrease of the lattice distortion approaching a hexagonal structure [5]. The existence of in-plane anisotropy shows that while the rotator phases lack long-range rotational order, they have well defined rotational potential minima with respect to the lattice directions. The (more slowly) decreasing $\Delta\chi$ with increasing T is consistent with the picture of the rotator phases where near-chain-end gauche bonds proliferate with increasing T [6].

In summary, we have determined the alignment of pure and mixed unfunctionalized n-alkane crystals in a magnetic field. We have quantified the orientational distribution in terms of competition with Brownian rotational motion showing scaling with field and crystal size, measuring both the longitudinal and transverse anisotropies. We have shown that the long axis of the molecule always aligns $\perp$ to the field and the carbon backbone plane tends to be $\perp$ to the field. The anisotropy is such that only a 2000 G field is required to orient $1\,\mu^3$ crystals such that 75% of the layer normals would be within 30° of $\perp$ to $\vec{H}$ at any given time. This corresponds to a nematic order-parameter [9] $s \equiv (3\langle\cos^2\theta\rangle - 1)/2 = -0.22$, where $s = -0.5$ is full antinematic order. While this work does not purport to verify claims of, or suggest a specific mechanism for ''magnetic conditioning'' to prevent wax deposition problems, it provides a needed scientific basis for discussion of magnetic interactions with wax crystals [13]. Our technique can be generally applicable to measuring anisotropies of soft material's susceptibilities, where growing and maintaining large single crystals may be difficult. By relating the molecular magnetic anisotropy to that of the lattice, the details of the rotational orientational distribution with respect to the lattice in various rotator phases can be studied.

We gratefully acknowledge discussions with H. E. King, Jr., K. S. Liang, J. J. Wang, H. Strey, J. Wang, and D. A. Weitz, and the technical assistance of S. Bennett and A. Mingino. The NSLS at BNL was supported by the DOE under Contract No. DE-AC02-76CH00016.

[1] A. Müller, Proc. R. Soc. London, Ser. A **138**, 514 (1932); A. A. Schaerer *et al.*, J. Am. Chem. Soc. **77**, 2017 (1955).
[2] C. W. Bunn, Trans. Faraday Soc. **35**, 482 (1939).
[3] D. Turnbull and R. L. Cormia, J. Chem. Phys. **34**, 820 (1961).
[4] B. Ewen, G. R. Strobl, and D. Richter, Faraday Discuss. Chem. Soc. **69**, 19 (1980).
[5] J. Doucet, I. Denicolo, and A. Craievich, J. Chem. Phys. **75**, 1523 (1981); G. Ungar, J. Phys. Chem. **87**, 689 (1983).
[6] R. G. Snyder *et al.*, Science **214**, 188 (1981); J. Phys. Chem. **97**, 7342 (1993).
[7] E. B. Sirota *et al.*, J. Phys. Chem. **99**, 798 (1995); E. B. Sirota, Langmuir **13**, 3849 (1997).
[8] J. C. Earnshaw and C. J. Hughes, Phys. Rev. A **46**, 4494 (1992); X. Z. Wu *et al.*, Science **261**, 1018 (1993).
[9] P. G. DeGennes and J. Prost, *The Physics of Liquid Crystals* (Clarendon, Oxford, 1993).
[10] G. Maret and K. Dransfeld, Physica **86–88B**, 1077 (1977); J. Seelig, F. Borle, and T. A. Cross, Biochim. Biophys. Acta **814**, 195 (1985); C. R. Sanders and J. H. Presegard, Biophys. J. **58**, 447 (1990); J. Katsaras *et al.*, Phys. Rev. Lett. **78**, 899 (1997).
[11] F. Scholz, E. Boroske, and W. Helfrich, Biophys. J. **45**, 589 (1984).
[12] I. Sakurai *et al.*, Proc. Natl. Acad. Sci. USA **77**, 7232 (1980).
[13] G. McWilliams, *Business Week* Oct. 30, 1995, pp. 75 and 76; W. Biao and D. Lijian (Soc. for Petrole, Engin); R. F. Benson *et al.*, *Chemtech*, April 1997, pp. 34–38.
[14] J. Farquharson and M. V. C. Sastri, Trans. Faraday Soc. **33**, 1472 (1937).
[15] G. H. Meeten, J. Chim. Phys. **69**, 1175 (1972).
[16] D. W. Davies, Mol. Phys. **6**, 489 (1963).
[17] T. G. Schmalz, C. L. Norris, and W. H. Flygare, J. Am. Chem. Soc. **95**, 7961 (1973).
[18] K. S. Krishnan, B. C. Guha, and S. Banerjee, Philos. Trans. R. Soc. London, Ser. A **231**, 235 (1933); K. Lonsdale, Proc. R. Soc. London, Ser. A **171**, 541 (1939).
[19] J. Bibette, J. Colloid Interface Sci. **147**, 474 (1991).
[20] R. Oldenbourg and W. C. Phillips, Rev. Sci. Instrum. **57**, 2362 (1986).
[21] B. J. Berne and R. Pecora, *Dynamic Light Scattering* (Wiley, New York, 1976).
[22] This error bar is mainly due to a 10% possible systematic uncertainty in the average size from the hydrodynamic radius measured by DLS [Ref. [21]]. The relative error between measurements and different samples is significantly smaller than this (i.e., ± 0.4).
[23] S. C. Nyburg, F. M. Pickard, and N. Norman, Acta Crystallogr., Sect. B: Struct. Crystallogr. Cryst. Chem. **B32**, 2289 (1976).